FORMING SIMULATION OF COMPOSITES WITH THERMO-VISCOUS PROPERTIES

Martin Schulz[1], Jens Lüke[2]

[1]Dassault Systemes Deutschland GmbH, Joseph-Wild-Str 20, 81829 Munich, Germany
Email: martin.schulz@3ds.com, Web Page: http://www.3ds.com
[2]Dassault Systemes Deutschland GmbH, Elisabethstrasse 16, 52062 Aachen, Germany
Email: jens.lueke@3ds.com, Web Page: http://www.3ds.com

Keywords: thermoforming, thermo-viscous, MAI Form, anisotropic friction

Abstract
MAI Form is one of several projects of the MAI Carbon cluster initiative, which is focused on the large-scale industrial usability of carbon reinforced plastics. As one part of MAI Form, the simulation of a thermoforming process including the springback calculation should be improved. The complete simulation chain, starting with the thermoforming process and ending with mapping the results like fiber orientation and thicknesses to the structural simulation models, should be built in Abaqus. The most challenging part in the simulation chain is the analysis of the deep drawing process. To improve the accuracy of these simulation, a thermo-visco-elastic-plastic material model as well as an anisotropic "sticky" contact model were needed. Therefore, the Abaqus on-board functionalities were extended with user subroutines for the material and contact behavior. The status quo of the simulation chain which has been achieved so far during this ongoing project is shown. It starts with the selection of the material modeling approach. The second part discusses the modeling of anisotropic contact. The deep drawing process necessitates a finite sliding contact approach that accounts for the influence of the momentary fiber orientations of both plies in contact relative to the sliding direction.

1. Introduction

MAI Form is a project in the framework of MAI Carbon focused on improving the predictability for forming of materials with thermo-viscous constitutive and interface properties. The main objective is improving the methods of material characterization, simulation and validation. The simulation of the complete workflow including the spring back calculation after cooling should be done with Abaqus Unified FEA.
Forming simulations for sheet metals or dry preforms are state of the art since years. To achieve improvements in simulation methods, this state of the art modeling approaches needs to be extended in order to handle the thermo-viscous behavior. Therefore, a proper constitutive law, an anisotropic viscous and "sticky" contact model and a fully couple temperature-displacement simulation procedure is needed. While the last one is fully available in Abaqus Unified FEA environment, the material constitutive material model and the contact model needs to be defined via user subroutines. The content of the user subroutines are briefly described in this paper.

Excerpt from ISBN 978-3-00-053387-7

2. Material Constitutive Model

The material model must be able to describe nonlinear thermo-viscoelastic and elastic-plastic behavior up to a strain of 25% in a temperature range between room temperature and 280 °C. Beside the technical requirements, there a practical ones as well. Obviously, it must be easy to use and should only request a minimum number of input parameter which need to be identified in simple tests.

2.1. Rheological Model

In [1] a variation of the K-BKZ-model (Kaye - Bernstein, Kearsley, Zapas) was used for thermoforming simulations of non-reinforced thermoplastics with reasonable results. This model consists of a series of spring-damper combinations, a so called Prony series, which defines the viscoelastic behavior as described in 2.1.1. Each term of the Prony series is characterized by a relaxation time τ. This model was extended with a temperature dependency of the relaxation time and an elastic-plastic part to match the needs of the MAI Form project. The rheologic scheme of the visco-elastic, elastic-plastic material model is shown in figure (Fig. 1). The stress tensor (Eq. 1) at any material point in the model can be written as the sum of the visco-elastic stress $\underline{\sigma}_{ve}$, the elastic-plastic stress $\underline{\sigma}_{epl}$ and a contribution from carbon fiber reinforcement $\underline{\sigma}_{fib}$.

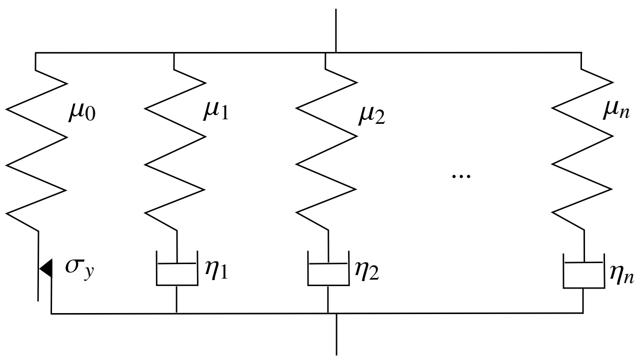

Figure 1. Rheologic model

$$\underline{\sigma}(t) = \underline{\sigma}_{ve}(t) + \underline{\sigma}_{epl}(t) + \underline{\sigma}_{fib}(t) \tag{1}$$

2.1.1. Visco-elastic Part

The visco-elastic part of the stress (Eq. 2) follows Wagner's variation of K-BKZ model according to [2].

$$\underline{\sigma}_{ve}(t) = \int_{-\infty}^{t} m(t-t') \cdot h(I_1, I_2) \cdot \underline{C}(t,t')\, dt. \tag{2}$$

The first term of the integral in (Eq. 2) is the memory function (Eq. 3) with the material dependent relaxation time τ_i and stiffness μ_i of the i-th Prony term.

$$m(t-t') = \sum_i \frac{\mu_i}{\tau_i} \cdot \exp\left(-\frac{t-t'}{\tau_i}\right). \tag{3}$$

The second term is the Finger strain tensor which describes all past configurations $x(t')$ relative to the current configuration $x(t)$ and reads as

$$\underline{C}(t,t') = \underline{F}^{-1} \cdot \underline{F}^{-T} = \left(\frac{\partial x(t')}{\partial x(t)}\right)^{-1} \cdot \left(\frac{\partial x(t')}{\partial x(t)}\right)^{-T}. \tag{4}$$

Excerpt from ISBN 978-3-00-053387-7

Finally, the third term is the so called damping function proposed by Wagner which introduce nonlinearity for large strains. In this paper, we use the Wagner II form (Eq. 5), a function of the first and second invariants I_1 and I_2 of the Finger strain tensor.

$$h(I_1, I_2) = \frac{\mu(t, I_1, I_2)}{\mu(t)} = \frac{1}{\exp\left(\beta \cdot \sqrt{\alpha \cdot I_1 + (1-\alpha) \cdot I_2 - 3}\right)} \tag{5}$$

Within a small temperature range a linear variation of the relaxation time is typically assumed for thermo-rheologic simple materials. In MAI Form the temperature vary between 280°C during forming simulation and room temperature during spring back calculation. Thus, the thermo-rheologic simplicity is not given. From forming to springback calculation, the material pass through the melting temperature Θ_m and the glass transition temperature Θ_g and by that, the behavior change from ductile above Θ_m to rubber elastic between Θ_g and Θ_m and finally brittle and "glassy" below Θ_g. While the transition from ductile to elastic behavior is handled by the elastic-plastic part of the constitutive law in 2.1.2 the transition through Θ_g results in a almost infinite viscosity. This effect is written in the Vogel-Fulcher-Equation (Eq. 6) which leads to a temperature dependent relaxation time (Eq. 7). In (Eq. 6 and 7) B is a material dependent parameter which describes the shape of the transition, η_0 is the viscosity at infinite temperature and Θ_0 is the temperature at which the viscosity becomes infinite.

$$\eta = \eta_0 \cdot \exp\left(\frac{B}{\Theta - \Theta_0}\right) \tag{6}$$

$$\tau_i(\Theta) = \frac{\mu_i}{\eta_i} = \frac{\mu_i}{\eta_0 \cdot \exp\left(\frac{B}{\Theta - \Theta_0}\right)} = \frac{\tau_i^0}{\exp\left(\frac{B}{\Theta - \Theta_0}\right)} \tag{7}$$

Figure (Fig. 2) shows exemplary the variation of the storage modulus vs. temperature for a material according to figure (Fig. 1) which results from the temperature dependent relaxation time.

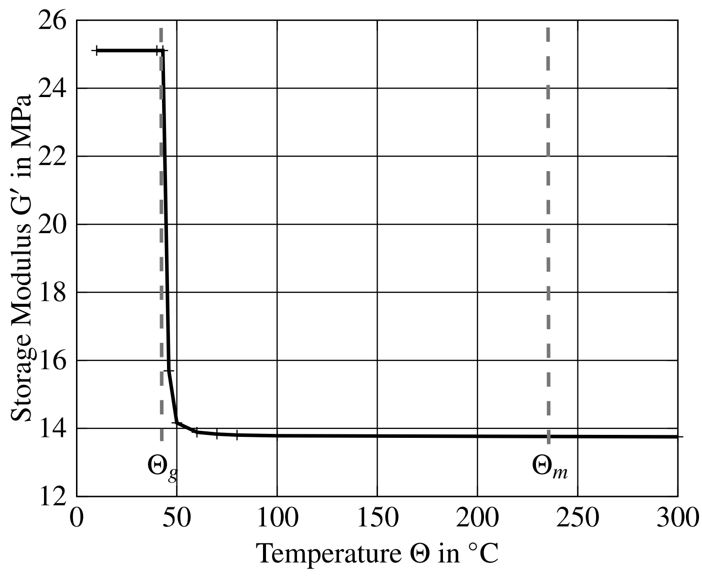

Figure 2. Storage Modulus vs. Temperature

2.1.2. Elastic-plastic part

During the forming simulation, the temperatures will be above the melting temperature Θ_m. Thus, the finite deformations will be in the ductile material state while during spring back calculations at temper-

Excerpt from ISBN 978-3-00-053387-7

atures below Θ_m only small elastic strains are expected. With this assumptions, a small strain elastic-plastic material model was selected for convenience. Similar to the metal plasticity, a Mises-plasticity model with linear isotropic and kinematic hardening was implemented. The advantages of this model is the limited number of required parameters. It requires at least 1 parameter (σ_y) for ideal plastic behavior and at most 3 parameter for fully linear kinematic (H) and isotropic ($\hat{H}$) hardening. The yield criterion is given with equation (Eq. 8) [3].

$$f = \left\| \underline{S} - \underline{q} \right\| - \sqrt{\frac{2}{3}} \cdot \sigma_y(\Theta) - \hat{q} \leq 0 \tag{8}$$

The first part in (Eq. 8) is the euclidean norm of the deviator stress $\underline{S}$ minus the backstress tensor $\underline{q}$ which describes the kinematic hardening according to equation (Eq. 9). The third part is the isotropic hardening following the equation (Eq. 10)

$$\underline{q} = -\frac{2}{3} H \cdot \underline{\alpha} \tag{9}$$

$$\hat{q} = -\hat{H} \cdot \hat{\alpha} \tag{10}$$

The temperature dependency of the yield stress σ_y in (Eq. 11 and 12) is similar to the Johnson-Cook plasticity model [4]. The main difference is, that the yield stress σ_y did not drop to zero above the melting temperature Θ_m but to a small fraction k_y of its initial value σ_{y0}. In addition to k_y, σ_{y0}, the melting temperature Θ_m and transition temperature $\Theta_{transition}$ must be provided. The later parameter defines the lower boundary of the temperature range in which the yield stress drops.

$$\sigma_y(T) = \sigma_{y0} \cdot \left(k_y + \left(1 - k_y\right) \hat{\Theta} \right) \tag{11}$$

$$\hat{\Theta} = \begin{cases} 0 & \text{for} \quad \Theta < \Theta_{transition} \\ (\Theta - \Theta_{transition}) / (\Theta_m - \Theta_{transition}) & \text{for} \quad \Theta_{transition} \leq \Theta \leq \Theta_m \\ 1 & \text{for} \quad \Theta > \Theta_m \end{cases} \tag{12}$$

2.1.3. Stiffness contribution from Fiber reinforcement

The visco-elastic and elastic-plastic stress contributions in the previous sections describe the material constitutive law for the thermoplastic matrix. The focus of MAI Form is the thermoforming simulation of carbon fiber reinforced thermoplastics which requires additional terms for the reinforcements. As the strain in the fibers can be considered as small, a simple linear elastic stress-strain relationship was used.

$$\underline{\sigma}_{fib}(t)_{i,i} = E_i^{fib} \cdot \left(\underline{\epsilon}_{el} \right)_{i,i} \tag{13}$$

The characterization of the material was done for the uni-directional layers only. In that case, the Young's modulus in fiber direction E_1 is required while the tensile stiffness perpendicular to the fibers can be neglected and the compressive transversal stiffness is by 2-3 orders less then E_1. To prevent an overestimation of the bending stiffness, the stress contribution from the fiber reinforcement are added only at the mid-plane of the elements.

2.2. Parameter evaluation

In order to test the user defined material described above, an example material with linear visco-elastic properties based results from [1] was fitted. In case of linear visco-elasticity, the shear modulus μ_i in the i-th Prony term at given relaxation time τ_i can be estimated as

$$\mu_i \approx \ln\left(\frac{\tau_i}{\tau_{i+1}}\right) \cdot \frac{2}{\pi} \cdot G''\left(\omega = \frac{1}{\tau_i}\right) \tag{14}$$

Excerpt from ISBN 978-3-00-053387-7

With the results of the estimation, a one-element simulation was performed with the material constitutive law described in chapter 2.1. The complex shear modulus of test, pre-estimation and simulation vs frequency are shown in figure (Fig. 3). Similar results could be obtained for bending test and non-linear visco-elastic behavior not shown here.

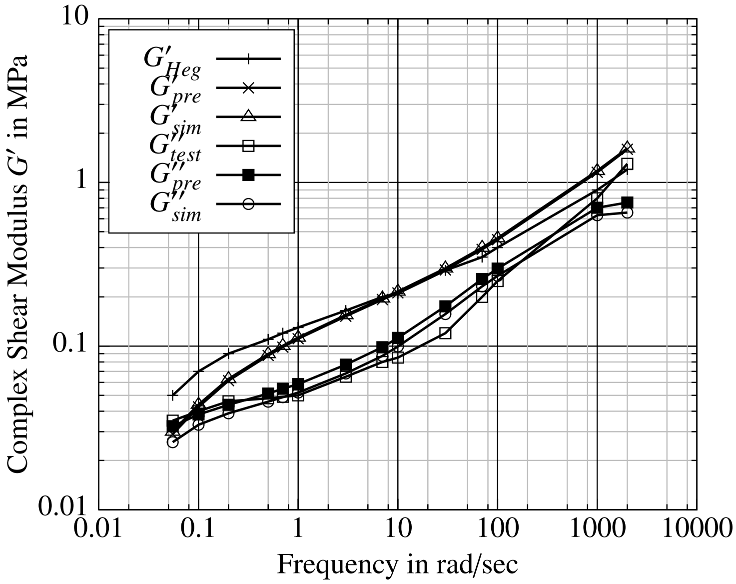

Figure 3. Complex shear modulus from test, pre-estimation and simulation

3. Contact modeling

3.1. Built-in capabilities of the Abaqus solver

The current release of Abaqus at the time of this conference allows to model anisotropic contact between a structured (non-isotropic) slave surface and a non-structured (isotropic) master surface with the implicit solver (Abaqus/Standard). Only the orientation of the slave surface is taken into account for this contact formulation. The explicit solver (Abaqus/Explicit) has no built-in capability to model anisotropic contact. "Sticky", i.e. viscoplastic contact conditions due to thermoplastic contact surface material properties cannot be handled by any built-in contact model. Due to the rapid and complex evolution of contact conditions during the forming process, only the explicit solver is considered for this study. The user subroutine interfaces available for contact interaction modeling with the explicit solver do not provide information regarding the present orientation of the contacting surfaces.

3.2. Goals within the MAI Form project

With regard to explicit contact modeling, the authors are working on implementing a contact modeling technique using Abaqus/Explicit user subroutine interfaces that should allow to account for the following characteristic aspects:

- The friction force depends on the spatial orientation of both structured surfaces and the direction of relative movement of the two surfaces.
- In the case of large shear deformations of the plies, the actual direction of the uniaxial fibres should

be determined, as the friction properties depend on the orientation of the uniaxial fibres in both surfaces with respect to the relative displacement direction.

- The contact modeling technique should allow to mesh the plies independent of the fiber direction.
- The contact modeling technique should work independently of the material model chosen for the plies.

3.3. Contact implementation

The data flow of the current implementation of anisotropic contact created as part of the MAI-Form project is depicted in figure (Fig. 4) The components of the initial fiber direction vector are stored as three scalar field variables at the nodes. The momentary fiber direction is computed in user subroutine VUFIELD using the initial fiber direction vector and the rotational degrees of freedom of the nodes. The individual plies are modeled using continuum shell elements, because stacking conventional shell

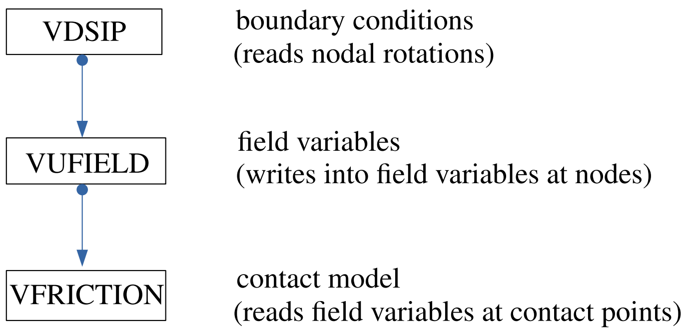

Figure 4. Data flow between user subroutines used for anisotropic contact

elements with relevant shear stresses at the contact interfaces would lead to numerical problems due to the offset between the ply surface and the node location. Shell or beam elements with small stiffness therefore have to be added on the surfaces of the continuum shell elements to create rotational degrees of freedom at the nodes (Fig. 5 and 6). The nodal rotations are currently not provided in the VUFIELD

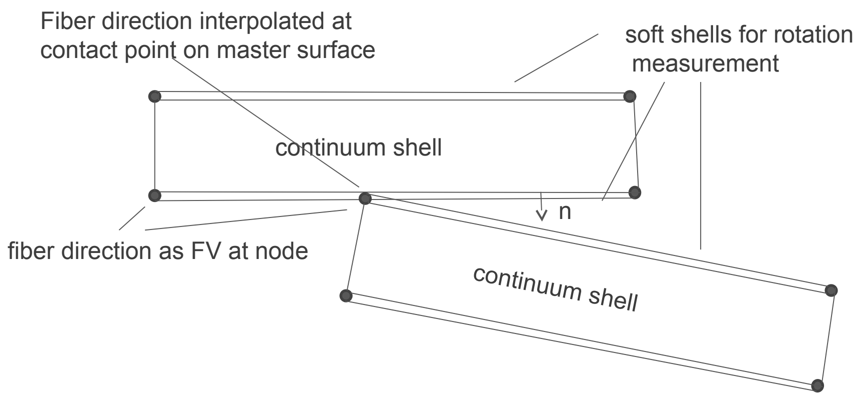

Figure 5. Using shell skins to measure rotations

interface. They can be accessed in a boudary condition user subroutine VDISP instead and transferred to VUFIELD via a common allocatable array. This procedure is possible, because VDISP allows to read nodal degrees of freedom (displacements and rotations) for all nodes for which a user-defined boundary

Excerpt from ISBN 978-3-00-053387-7

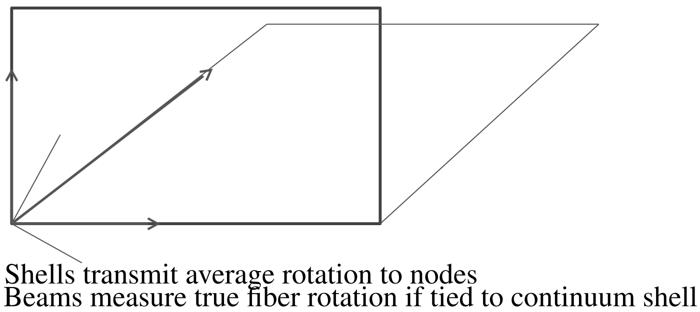

Figure 6. Shells vs. beams to measure rotations

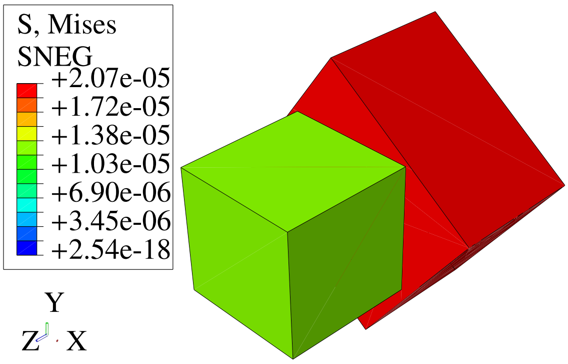

Figure 7. Block model for anisotropic contact verification

condition is specified. If values are not assigned to the degrees of freedom during this process, the nodes are actually not restrained and the nominal boundary condition has no effect on the analysis results.

3.4. Anisotropic contact model

The assumption of anisotropic contact behavior has two effects on the analysis results: The contact force parallel and resisting to the relative tangential movement of both surfaces varies with the angles between relative movement and fiber direction on both surfaces, and there is in general a non-zero friction force component normal to the direction of relative movement, but in the plane of contact. The anisotropic contact model is currently programmed using the VFRICTION user subroutine interface. Since the test results for anisotropic friction for the materials investigated in the MAI Form project are not yet available, no specific constitutive interaction model is implemented. The friction coefficients parallel and normal to the relative sliding direction are instead entered in a table as a function of the two angles between the fibre directions in both surfaces and the relative sliding diretion. In addition, a cohesion can be specified that describes the shear force that can be transmitted with zero normal stress.

3.5. Block model example

A simple model of two blocks in contact is used to verify the model for different displacement and rotation paths (Fig. 7). Both blocks consist of one brick element with an added shell element skin in the contact surface to measure nodal rotations. The contact surfaces are both specified rigid to allow the definition of exact displacements using boundary conditions. A purely normal displacement is applied at first, followed by alternating translations and rotations. While the shear forces in the direction of relative

Excerpt from ISBN 978-3-00-053387-7

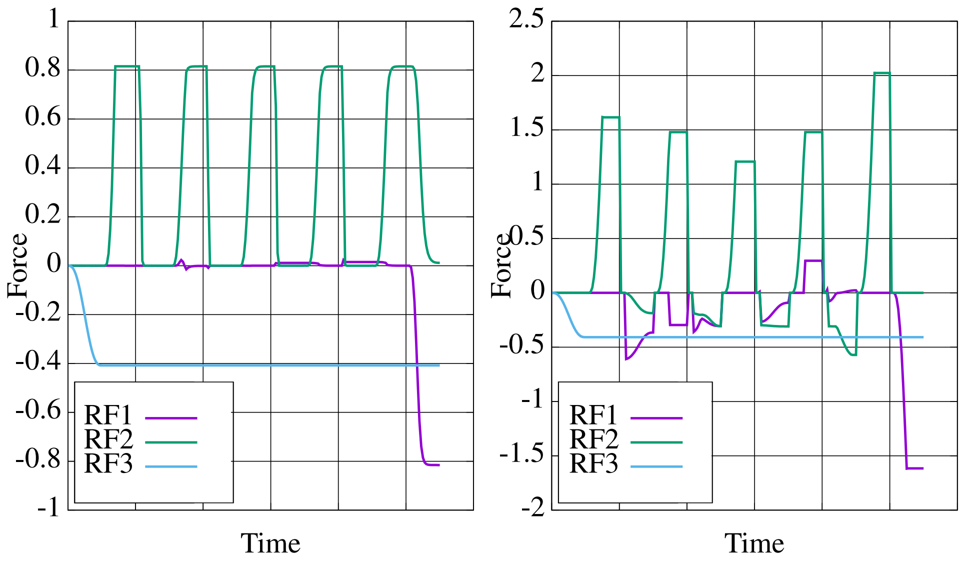

Figure 8. Time history of reaction forces for isotropic (left) and anisotropic (right) contact

movement are bounded by the same maximum value in the isotropic example, the maximum shear stress changes with the changing orientations in the anisotropic case (Fig. 8). For this case, the lateral shear forces normal to the relative sliding direction also become apparent.

3.6. Next steps within the MAI Form project

Further work will concentrate on describing the viscoplastic contact behavior, including the normal strength in tension, as a function of temperature. Also, an approach to determine the nodal rotations from the integration point strains and orientations will be attempted to avoid the necessity to add shell or beam elements with small stiffness to measure the rotations.

Acknowledgments

We would like to thank the German "Bundesministerium fpr Bildung und Forschung" funding this project as well as all project partner in MAI Form.

References

[1] B. Hegemann. *Deformation von Kunststoffen beim Thermoformen -experimentelle und virtuelle Bestimmung-*. PhD thesis, Universitt Stuttgart, 2004.

[2] Evan Mitsoulis. 50 years of the k-bkz constitutive relation for polymers, 2013.

[3] P. Wriggers. *Nichtlineare Finite-Element-Methode*. Springer, 2001.

[4] *Abaqus Analysis User's Guide*.

Excerpt from ISBN 978-3-00-053387-7